Science and Engineering Research Council
Rutherford Appleton Laboratory
Chilton DIDCOT Oxon OX11 0QX

RAL-93-028

Rotational Tunnelling Spectroscopy with Neutrons

C J Carlile and M Prager

April 1993

ROTATIONAL TUNNELLING SPECTROSCOPY WITH NEUTRONS

C. J. CARLILE

ISIS Pulsed Neutron Facility, Rutherford Appleton Laboratory
Chilton, Oxfordshire, OX11 0QX, UK.

and

M. PRAGER

Institut für Festkörperforschung, KFA Jülich, Postfach 1913
D-5170 Jülich, Germany.

Neutron tunnelling spectroscopy has been a very fruitful field for almost two decades and is still expanding into new areas, both experimentally and theoretically. The development of the topic is reviewed from the theoretical point of view, highlighting new approaches, and selected examples of more recent experimental work are presented. A brief discussion of instrument performance and experimental requirements is given.

1. Introduction

The first measurements to be published on quantum molecular tunnelling using inelastic neutron spectroscopy[1,2] were carried out at the Jülich reactor and appeared in 1975 at a time when the high flux reactor at the Institut Laue-Langevin had just started its user programme. The ILL was furnished with a suite of high resolution neutron spectrometers[3] of such advanced design that the preliminary pioneering work at Jülich was able to be amplified over the following decade into a subject in its own right which, from the quality and precision of its results, was able to rank beside phonon spectroscopy and magnetic diffraction as examples of the unique power of the neutron as a probe of condensed matter.

In recent years the applicability and range of the method has been extended with the advent of pulsed neutron sources, notably ISIS in Britain and KENS in Japan, where high resolution spectrometers[4,5] using white beam techniques have provided different insights into the subject. This development was all the more unexpected since pulsed sources have been until quite recently perceived as sources of high energy neutrons rather than the cold neutrons necessary to achieve the microelectronvolt resolutions required for tunnelling spectroscopy.

The field was first reviewed in 1981 in a monograph[6] which emphasised the isolated single-particle character of molecular rotation. The theory of neutron spectroscopy of tunnelling molecules was presented for one-dimensional rotors such as CH_3 groups and NH_3, and three-dimensional rotors such as CH_4 and NH_4^+.

At about that time a series of biennial conferences was started, one of which was published in 1986[7] which records the progress in the subject up to then. Whilst the experiments in the early years were aimed at a basic understanding of the phenomenon and towards determining rotational potentials in relatively simple molecular crystals, the second period was devoted to more complex problems including the direct coupling between two methyl groups,[8] the coupling of the quantum rotor to phonons in the solid[9]

To be published in:
"Condensed matter and materials science with neutron beam techniques"
Editors: U Dahlborg and S W Lovesey
International Journal of Modern Physics B

(which determines the temperature dependence of the phenomenon) and the study of tunnelling as a function of pressure.[10-12] A tunnelling atlas compiled at that time[13] gives an almost complete review of materials studied up to 1987. Reviews of the topics of vibrational dynamics of hydrogen molecules in unusual chemical environments,[14] matrix isolation spectroscopy of tunnelling entities,[15] and a general review covering all important aspects of tunnelling,[16] have been presented in a special edition of Spectrochimica Acta (1992).

There has been a trend in the past few years towards the study of chemically more complex materials, matrix isolated molecules,[17-21] mixed systems,[22-29] clathrates and inclusion compounds,[30-31] molecules on surfaces[32-35] and in intercalates,[36-40] and those samples which exhibit coupling. This trend has been facilitated by the availability of high precision spectrometers and a concentration upon high resolution studies in the microelectronvolt energy transfer region which have often revealed unexpectedly complex structured spectra. The theories covering two coupled methane molecules,[41] more than two coupled uniaxial rotors, and different forms of coupling have been considered,[24,41-49] and corresponding experiments have been performed.[24-27,47-49] Coupling effects are especially pronounced for systems with weak single particle potentials. The coupling to phonons appears to have found a final, generally valid description[50-53] which allows a detailed understanding of the experimental findings.[54-56] The influence of various types of disorder has also been studied.[18-19,57-58] One of the original aims of tunnelling spectroscopy - the determination of interaction potentials in molecular solids - has obtained a new quality by combining spectroscopy and high-precision diffraction studies[59-60] which allows an independent test of the reliability of pair interaction potentials to be carried out. The simultaneous observation of inelastic spectra and sections of the diffraction pattern on the IRIS spectrometer has proved to be very helpful in interpreting data from samples prepared uniquely in-beam.[37,40]

Finally, neutron tunnelling spectroscopy yields detailed information on spin conversion. For CH_4, a theory had already been developed quite early on to explain NMR results,[61] whereas this was only achieved quite recently for CH_3 groups.[62-63] This topic has not been widely studied experimentally except for detailed measurements using transmission geometry.[64-65]

2. Theoretical Background

2.1 *Single particle rotations*

The quantised rotational energy levels of a molecule, which has a rotational constant B given by

$$B = \frac{\hbar^2}{2I} \tag{1}$$

where I is the moment of inertia, are generally calculated under the assumption that the environment can be represented by a potential $V(\omega)$. This approximation is called The Single Particle Model. The rotor levels are then given by the solution of Schrödinger's equation with the Hamiltonian

$$H = B\nabla^2 + V(\omega). \tag{2}$$

In the case of rotation about a single axis (1-dimensional or uniaxial) there is only one characteristic angle $\omega = \varphi$ and $\nabla^2 = -\partial^2 / \partial\varphi^2$. The symmetry of the rotational potential clearly cannot be lower than that of the rotor and so, in the case of methyl groups, the potential is expanded into the following Fourier series

$$V(\varphi) = \sum_{n=1}^{N} \frac{V_{3n}}{2}(1 - \cos(3n\varphi - \varphi_{3n})) \qquad (3)$$

where φ_{3n} is a constant angular offset. This series is often truncated at the second term. When a higher symmetry of the surroundings imposes itself on the rotor, the leading term in the potential could be of higher order.[19,30,66] In the simplest case of a pure 3-fold potential we obtain

$$H = -B\frac{\partial^2}{\partial\varphi^2} + \frac{V_3}{2}(1 - \cos 3\varphi). \qquad (4)$$

Note that V_3 is the peak to peak height of the potential as illustrated in figure 1.

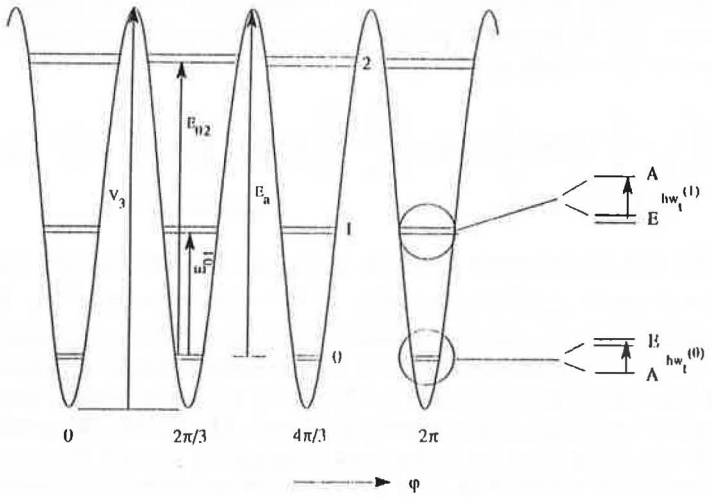

Figure 1. A representation of the energy levels of a CH_3 group in a 3-fold potential following Horsewill.[16] Note that the barrier height V_3 is expressed as the peak to peak amplitude. The activation energy E_a and the librational energies E_{0n} are indicated, together with the tunnel splittings.

This form of expressing the potential is a convention which unfortunately has not been adhered to consistently in the literature. Some papers, particularly those which treat the question of coupling rather than the single particle approach, express the potential as $V_3 cos3\,\varphi$, and consequently there is a phase difference of $\pi/3$, and a factor of two difference in the numerical value of V_3 between these two conventions. In order to remain consistent with the majority of *original papers* we have decided in this review to present single particle models with the former convention and coupling models with the latter convention.

The energy levels of the corresponding Schrödinger equation can then be described as a sequence of librational levels (at meV energies) which are tunnel split (by μeV), as indicated in figure 1. The tunnel splitting is extremely sensitive to weak changes of the potential.[6] For tetrahedral molecules the asymptotic behaviour at large potentials $V > 30$ meV can be represented by an exponential decrease[67]

$$\hbar\omega_t = \beta \exp\left(-\alpha\sqrt{V/B}\right) \qquad (5)$$

A similar relationship is valid for 1-dimensional rotors. The values of α (normally ~*1*) and β (normally ~*B*)[67] are characteristic of the type of rotor and the shape of the potential. It is this feature which makes tunnelling spectroscopy particularly attractive amongst all other methods of molecular spectroscopy.

Eq. (5) clearly shows that there exists a uniquely strong *isotope effect* for tunnelling transitions compared to other lattice modes. For example, in the harmonic approximation a librational mode E_{01} is reduced by $\sqrt{2}$ on deuteration, two being the ratio of the rotational constants. In the case of tunnelling this factor of $\sqrt{2}$ appears in the argument of the exponential function, which therefore amplifies the effect significantly, making the tunnelling frequency decrease disproportionately with increasing potential strength. For example at V=15meV the tunnel splitting is reduced by an order of magnitude with deuteration. At V=40meV this factor has reached 30. Thus the manifestation of a strong isotope effect represents an unambiguous proof of tunnelling.

The scattering function for neutrons from these rotors is most easily derived for protons, which are assumed to be located at points, and, for a polycrystalline material with equally populated tunnel states, reads as follows

$$S(Q,\omega) = \underbrace{\left(\frac{5}{3}+\frac{4}{3}j_o(Qd)\right)\delta(\omega)}_{\text{Elastic term}} + \underbrace{\left(\frac{2}{3}-\frac{2}{3}j_o(Qd)\right)\left\{\delta(\omega+\omega_t)+\delta(\omega-\omega_t)\right\}}_{\text{Inelastic term}} \qquad \text{.....(6)}$$

where Q is the momentum transferred to the neutron in the scattering process and d is the proton-proton distance. $j_o(Qd)$ is the spherical Bessel function and $\hbar\omega_t$ is the tunnel splitting of the librational ground state. Since in general no other excitations are found in the region, excitations detected in the μeV energy transfer range of a spectrometer are easily identified. Their character can be confirmed by raising the sample temperature to ~ 50K when the spectral lines will normally disappear. Should the integrated intensity of all observed tunnelling lines be lower than required by eq. (6) there could well be unresolved lines in the elastic peak. The probability of occurrence of crystallographically distinct tunnel rotors can then be estimated, resulting in structurally relevant information. The structure factors which determine the intensity variation with Q are different from eq. (6) if the leading term in the rotational potential is of sixfold symmetry.[68]

If a second rotational transition in figure 1 can be measured, for example the excitation E_{01} to the first librational state, then parameters of the rotational potential can be determined up to the second term in eq. (3). In general, a determination of any further terms is not worthwhile. Difficulties can arise if inequivalent methyl groups are present, making an unambiguous assignment of tunnelling and librational transitions to a particular rotor in the molecule or in the structure problematic.[69-70] Nevertheless a general experimental conclusion that the higher order terms in the potential are weak can be very helpful.[71] A number of multiline spectra containing tunnelling excitations of rational intensity ratios have found a simple explanation in this way.[69-70, 72]

The assumption that the protons are spatially localised at points in the strongly anharmonic rotational potentials can only be justified for small values of the momentum transfer $Q < 1\text{Å}^{-1}$. For larger Q the quantum mechanical proton density distribution ρ

$= \psi\psi^*$ modifies the structure factors given by eq. (6). Consequently the intensity variation of tunnelling lines with Q can give access to the wave function ψ itself. Such experiments have been performed for one-dimensional[73] and three-dimensional rotors.[20,74]

Molecules which contain methyl groups can be structurally rather complex and their crystallographic environment can be similarly complex. Accordingly the rotational potential can be decomposed into an intramolecular and an intermolecular term.

$$V(\varphi) = V_{\text{intra}}(\varphi) + V_{\text{inter}}(\varphi). \qquad (7)$$

The relative importance of the two contributions can be explored by investigating a molecule in various surroundings. In particular, results from the gas phase would yield the clearest answer by eliminating intermolecular contributions completely. Neutron spectroscopy however is presently only possible in dense phases for intensity reasons. Thus matrix isolation spectroscopy has proved to be very effective in determining the relative weights of the two interactions.[75]

In samples with dominant intramolecular interactions the tunnel splitting can be characteristic of the chemical neighbourhood of the rotating unit.[76] Therefore tunnelling spectroscopy can be used as a tool of chemical analysis. Certain materials do not show a significant intramolecular contribution to the rotational potential and are especially sensitive to the environment of the whole molecule. Some of these samples show interesting spectral effects due to intermolecular coupling.[24-25]

In a mean field model the potential experienced by the rotor globally represents its surroundings. The inter-rotor interaction can be split phenomenologically into three different components all of which vary as r_{ij}^{-n}, where r_{ij} represents the separation of the atoms i in the rotor from those j in the neighbouring molecules:

(i) **the attractive van der Waals' polarisation term**, which varies relatively weakly with distance and where $n=6$,

(ii) **steric repulsive forces**, which vary strongly with distance where $n>12$, and

(iii) **other electrostatic multipole forces**, with the exponent having a value $n=l+l'+1$, where l and l' represent the order of the interacting multipoles. If interactions are calculated between atoms, which represent monopoles, this is just the Coulomb interaction $(l=l'=0)$ with $n=1$. Often the molecule or the molecular rotor itself are treated as a unit. Then, depending upon the molecular symmetry, higher order terms become important, whilst for neutral units the Coulomb term of course vanishes. In the case of methane, for example, the first non-vanishing electrostatic moment is an octopole moment.

In many experiments pressure variation δp has been used to explore the dominant intermolecular interaction.[10-12,77-80] The reduction of intermolecular distances with pressure increases the rotational potential according to the relationship

$$V(\varphi,r) = V(\varphi,r_0).\left(\frac{r_0}{r}\right)^{n^*}. \qquad (8)$$

The main contribution to the potential comes from nearest neighbours. Detailed calculations show that atoms outside a sphere of order 3Å change $V(\varphi)$ by less than 5%. Despite not being equal to n, the effective exponent n^* is characteristic of the dominant

type of interatomic interaction. If we introduce the value of V from eq. (8) into eq. (5) we obtain, after some simple transformations

$$\delta\hbar\omega_t = C.n^* \frac{\delta r}{r} \tag{9}$$

The constant C contains only known quantities such as α and β of eq. (5), and the strength of the potential at zero pressure. Thus the only unknown is $\delta r/r$. Because there is commonly a lack of knowledge of crystallographic parameters with pressure, the variation of intermolecular distance with pressure is often derived from the isothermal compressibility κ of the sample.

$$\frac{\delta r}{r} = \kappa\delta p \tag{10}$$

In some cases[12,78] very large values of the exponent n have been determined, which emphasises the importance of steric hindrance in determining the potential barriers. In other cases[72,80] no shift of the tunnelling frequency, or even a shift to higher frequencies (implying a reduction in the strength of the potential barrier), is observed. This demonstrates that molecular solids often undergo more complex structural changes under pressure than would be concluded from the isothermal compressibility. Thus any deeper understanding requires an accurate knowledge of the variation of all structural parameters of the sample (lattice constants, all atomic positions etc.) for all experimental conditions. In principle this can be done on an instrument such as IRIS, which can carry out simultaneous diffraction scans, but this has yet to be attempted. Even a knowledge of the structure under standard conditions would allow direct access to the fundamentally important transferable pair potentials.[60]

In a more detailed calculation, the rotational potential is determined from the pair interactions V_{ij} and Coulomb interactions between the three protons i on the methyl group and their neighbours j

$$V(\varphi) = \sum_{i=1}^{3}\sum_{j=1}^{J}\{\ V_{ij}\left(r_{ij}(\varphi)\right) + \frac{e_i e_j}{r_{ij}(\varphi)}\ \}, \tag{11}$$

where e_i and e_j are the electrostatic charges. The pair potentials are often represented in the form of Born-Mayer potentials

$$V_{ij}\left(r_{ij}\right) = \alpha_{ij}\exp\left(\beta_{ij}r_{ij}\right) - \frac{\gamma_{ij}}{r_{ij}^6} \tag{12}$$

where α_{ij}, β_{ij} and γ_{ij} depend only upon the types of interacting atoms.

$V(\varphi)$, calculated according to eq. (11), is then parameterised according to eq. (3) and the calculated eigenvalues, obtained from the solution of the Schrödinger equation (2), can be compared with experiment. Similar calculations as a function of pressure would significantly improve the value and clarity of the results.

2.2. *Coupled rotors*

The single particle potential represents only those interactions which depend on the orientation of the rotor at the origin and the **distances** to the surrounding atoms. In this theory the quantum rotor is treated as an entity characterised by its centre of mass $\boldsymbol{R_i}$ and its orientation φ_i. Other atoms have a centre of mass but are assumed to have no degree of orientation.

For a more general framework, terms must be added to the potential which depend on both the orientation of the rotor at the origin and the **orientation** of the neighbouring molecules, as well as their separation. For the case of interactions between pairs of molecules one obtains a multipole expansion of the potential[6]

$$V(\varphi_i) = \sum_{j=1}^{N+M} V_{ij,1}(\varphi_i, r_{ij}) + \sum_{j=1}^{M} V_{ij,2}(\varphi_i, \varphi_j, r_{ij}) \qquad (13)$$

where M denotes the number of quantum rotors and N the remaining atoms. The distance between two constituents is $r_{ij} = |\boldsymbol{R_i} - \boldsymbol{R_j}|$.

In the simplest case of two coupled methyl groups, which are coaxially aligned, a model Hamiltonian, consistent with eq. (13), is given by

$$\begin{aligned} H &= H_1 + H_2 + H_{12} \\ H_i &= -B\frac{\partial^2}{\partial \varphi_i^2} + V_3 \cos 3\varphi_i, \quad i = 1,2 \\ H_{12} &= W_3 \cos 3(\varphi_1 - \varphi_2) \end{aligned} \qquad (14)$$

The convention defining the single particle and interaction potentials is not unique in the literature and often inconsistencies occur. In eq. (14) the convention is different from that used in eq. (3).

Depending on the sign of W_3 the interaction potential favours a staggered or an eclipsed configuration of the two methyl groups. The coupling leads to a splitting of the librational ground state into a quartet with four allowed transitions, observable in an inelastic neutron scattering experiment.[8] Lithium acetate is one of the most well-studied systems using neutron spectroscopy and a large amount of experimental data from this sample can be explained consistently is terms of isolated close-contact pairs of coupled methyl groups.[25] The Hamiltonian given in eq. (14) is a particular case of a more general problem which considers two coupled tops with non-parallel rotational axes.

The theory of coupled rotors has been extended to three interacting molecules,[44] and to even larger clusters.[45] However, only very recently, a theoretically clear and mathematically efficient method to treats up to four interacting molecules in a linear chain[46] has been developed. The calculation suggests that such coupling would cause a splitting of the tunnelling line itself which is not resolvable with the resolution of present instruments. Thus spectra could **look as if** they were due to a single isolated CH_3 group. The effect of coupling only rescales the tunnel splitting energy. The important conclusion of this work is, ironically, that even supposedly simple single-line tunnelling

spectra may be difficult to interpret. The observed tunnel **frequency** from a coupled system may be significantly different from that which would have been exhibited by the equivalent single rotor system and yet the line may remain identical in shape. In these cases interpreting the spectrum in terms of a single particle explanation may well be completely wrong.

The coupling of an infinite chain of rotors by nearest neighbour interactions has been developed using a novel approach.[24] The Hamiltonian for an infinite chain is given by

$$H = \sum_{j=1}^{\infty} \left\{ -B_j \frac{\partial^2}{\partial \varphi_j^2} + \tfrac{1}{2} V_3 \left(1 - \cos 3\varphi_j\right) + \tfrac{1}{2} V_c \left(1 - \cos 3(\varphi_{j+1} - \varphi_j)\right) \right\} . \quad (15)$$

It emerges that, after expanding the coupling term V_c to second order, this Hamiltonian is equivalent to that of the sine-Gordon potential. In addition to tunnelling excitations, the solution of the quantum sine-Gordon equation requires the existence of a further excitation, the quantised breather mode. A breather mode is represented as a bound pair of quasi-particles, a soliton and an anti-soliton, which propagates along an infinite one-dimensional chain of methyl groups without dissipation of energy. This theory has been applied successfully to the anomalous behaviour of the low energy excitational spectrum from 4-methyl pyridine, and also when it is diluted in its perdeuterated derivative, when the chain length is reduced by the presence of deuterated molecules.

Spectra of hydrogenated 4-methyl pyridine can also be described by a model of two dynamically coupled methyl groups.[47] In this case the sum of two single particle Hamiltonians, as given in eq. (2), is extended by a mixed derivative term

$$H = -B \frac{\partial^2}{\partial \varphi_1^2} - B \frac{\partial^2}{\partial \varphi_2^2} - B \frac{\partial^2}{\partial \varphi_1 \partial \varphi_2} + V_3 (\cos 3\varphi_1 + \cos 3\varphi_2). \quad (16)$$

The appearance of novel theories, not yet fully accepted by the majority, represents an exciting development in tunnelling spectroscopy which challenges accepted views and stimulates experimental investigations of more complex systems and reinvestigations of known samples with greater precision.

2.3. *Coupling to phonons*

The continuous transition from the discrete inelastic spectrum of quantum rotation at low temperature, to the manifestation of quasielastic broadening resulting from classical stochastic reorientation as the temperature increases, i.e. the transition from tunnelling to hopping known as the quantum-to-classical transition, has been one of the most enduring areas of study in rotational tunnelling. Experimentally it is found that the tunnelling lines broaden and shift with increasing temperature, usually towards the elastic line. The shift $\Delta\hbar\omega_t$ and width Γ_t follow Arrhenius dependencies

$$\begin{aligned} \Delta\hbar\omega_t &= \nu_0 \exp\left(-E_s / kT\right) \\ \Gamma_t &= \Gamma_0 \exp\left(-E_\Gamma / kT\right) \end{aligned} \quad (17)$$

The first comprehensive and consistent theory of the coupling of the quantum rotor to phonons, which was able to describe the observed shift *and* broadening of the tunnel lines, was given in 1982.[9] The problem was separated into an isolated rotor in a potential (single particle model) and a phonon bath, which were coupled in second-order perturbation theory. The theory describes, in a qualitatively correct manner, the broadening by a resonant coupling to phonons of energy E_{01}, thus $E_\Gamma \sim E_{01}$. The shifting is represented by an interaction with the so-called coupled density of states for all phonons with energies below E_{01}, thus $E_s < E_{01}$. Additionally it explains the appearance of a purely quasielastic component due to fluctuations of the E_a and E_b levels against each other. These levels are degenerate at low temperature. Despite the conditions of (i) weak coupling and (ii) low temperatures far below the transition to classical behaviour, the theory has found qualitatively valid applicability in many systems. Using a path integral method for phonon coupling at higher temperatures, consistency with the perturbation approach at low temperature has been demonstrated.[81]

Quite recently, by substituting the molecule and its surroundings by an array of harmonic oscillators, an exactly soluble formalism has been developed[53] the results of which are in agreement with those from the perturbational approach and are particularly valid for strongly coupled systems. Because of the simplicity of this model certain experimental observations are not reproduced. Since the groundstate consists of two non-degenerate levels, in contrast to methyl groups where the higher E-level is a degenerate doublet, the calculated scattering function does not contain a quasielastic component.

The precise width of the quasielastic line γ_{qe} is shown, both experimentally[54-56] and by computer simulation,[52] to be less than the width of the inelastic line γ_{in}. Calculations applying the Nakajima-Zwantzig theory[51] have provided an explanation of this observation. These various approaches towards the coupling of quantum rotors and phonons have recently been presented together with the most accurate experimental studies of this phenomenon.[54-55]

Insights into the general physics of a problem are often furnished with simple models. One such is the model Hamiltonian used for the case of rotor-phonon coupling

$$H = H_R + H_P + H_{RP}. \tag{18}$$

Where H_R, H_P and H_{RP} represent the rotor, the phonon (described as a harmonic oscillator) and the rotor-phonon interaction Hamiltonians respectively, which are given analytically as

$$\begin{aligned} H_R &= -B\frac{\partial^2}{\partial\varphi^2} + V_3\cos 3\varphi \\ H_P &= \frac{p^2}{2m} + \frac{1}{2}m\omega^2 x^2 \\ H_{RP} &= x\left(g_s \sin 3\varphi + g_c \cos 3\varphi\right) \end{aligned} \tag{19}$$

The first term in the equation for H_{RP} is called a 'shaking' component and the second term is a 'breathing' component. If H_R and H_{RP} are combined into an effective single particle potential, the shaking term causes an angular shift whilst the breathing term affects the barrier height. (This explains the chosen names). Increasing the sample temperature in order to populate phonon states increases the amplitude of the shaking term and leads to a

decrease of the observed tunnel splitting, whilst the breathing term would lead to an increase.

In methyl iodide[82] both effects are dominant over different temperature ranges, allowing the two components to be separately quantified as illustrated in figure 2. In most experimental cases the tunnel frequency is observed to fall with rising temperature, indicating that the coupling to shaking modes is dominant in general.

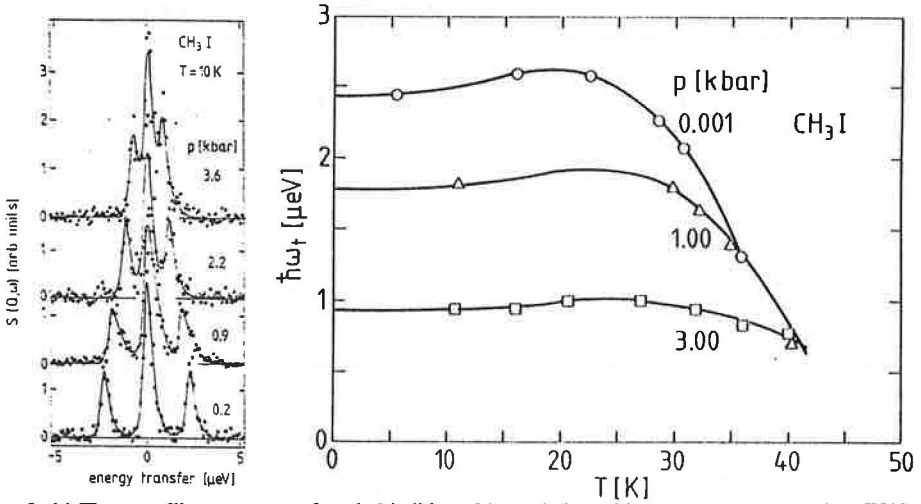

Figure 2. (a) The tunnelling spectrum of methyl iodide and its variation with pressure as measured on IN10 at ILL with a resolution of 0.3μeV. (b) The shift of the lines at various pressures as a function of temperature, showing an initial increase followed by the more usual decrease.[82]

Very recently a theory to explain the quantum to classical transition which is radically different from previous conceptual approaches has been developed.[83] This theory, which describes the coupling by gauge potentials and utilises the concept of trajectories and Berry's phase rather than energy levels, rests upon a unified theoretical treatment derived from other branches of physics rather than just condensed matter theory. It has been reviewed in some detail recently.[16]

2.4. *Time-dependent phenomena - spin conversion*

The equilibration of a rotor with its environment as the temperature falls involves spin flip transitions of the tunnelling molecules between levels of different symmetry. In the case of protons such transitions are mediated by the dipole-dipole interaction, and for deuterons by the electric quadrupolar interaction. The energy released is dissipated to the lattice by coupling to phonons. Because of the weakness of the dipole-dipole interaction conversion times are long, typically being many hours. The presence of a small quantity of a paramagnetic impurity such as oxygen can lead to a dramatic increase in conversion rate by many orders of magnitude.[63]

A theory of spin conversion in methane was satisfactorily developed a decade ago,[61] whereas a theory applicable to methyl groups was only obtained recently[62-63] in a model of intramolecular dipolar coupling. The coupling to phonons has been represented by the breathing and shaking modes of eq. (19). For the case of breathing modes a finite conversion time $t_c \propto \omega_t^4$ is predicted even at zero temperature. At the lowest temperatures the conversion rate proceeds linearly with temperature T, and at intermediate

temperatures as T^7 due to phonon scattering. Since the estimated conversion times in this model are very long (ca.100 days) it is questionable whether the observed effects[84-86] are due to this mechanism.

Transmission experiments[86] exploit the increase of total scattering with increasing total spin $<I(I+1)>$ of the molecule associated with its conversion into the A groundstate.[87] It works without energy analysis, and thus can only give reliable information provided that the system under study exhibits a single tunnelling line. Samples with inequivalent methyl groups or with complex sublevel structure need to be investigated by inelastic neutron scattering if complete and unambiguous results are required. Spin conversion spectroscopy is a relatively new topic which will certainly be explored more fully in the future. The transmission technique requires only low neutron fluxes and no advanced spectrometers and thus can be used on small reactors for the study of tunnelling phenomena.

3. Scientific Examples and Experimental Methods

3.1. *Scientific examples*

3.1.1. *Methyl tunnelling: nitromethane and tetramethyl lead*

Nitromethane represents one of the most well-studied materials by tunnelling spectroscopy. It contains only one type of CH_3 group in the orthorhombic unit cell, having space group $P2_12_12_1$ and 4 molecules per unit cell. Thus the tunnel spectrum contains one single line as seen in figure 3. The profile is resolution limited, which is interpreted as meaning that direct methyl-methyl interactions are negligible. The isotope effect,[80] the pressure dependence of the rotational levels,[72,80] and the influence of isotopic substitution,[29] have been investigated in both the tunnelling and the librational regions, and a potential consistent with all the data has been able to be extracted. This potential contains an uncharacteristically strong sixfold term. A first-principles calculation, on the basis of pair potential interactions,[59] was able to explain this potential remarkably well, but only by making the unusual assumption that *all methyl groups rotate in phase*. The system has been reviewed recently.[16]

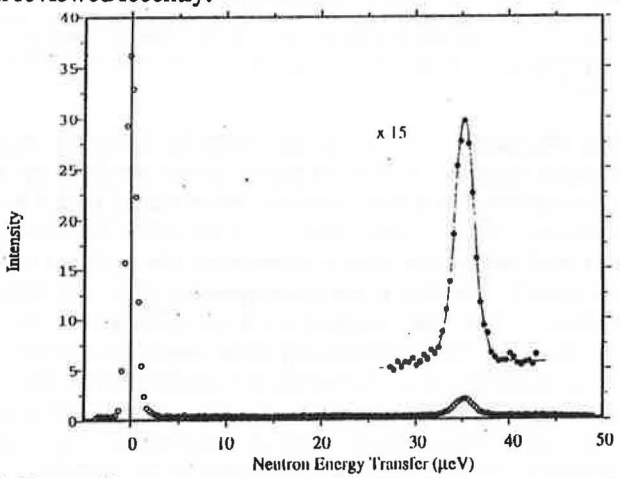

Figure 3. The single line tunnel spectrum of nitromethane at 35.4μeV at a temperature of 4.5K as measured on IRIS at ISIS with a resolution of 1.3μeV.[4] The spectrum was measured using mica analysers with a final energy of 208μeV (λ=19.8Å).

Tetramethyl-metal compounds represent the next most complex class of material, but they are nevertheless still simple. The molecule is a tetrahedron with a central metal atom and a methyl group at each apex. Tetramethyl tin is known to have a space group *Pa3* with a threefold axis at the molecular site[88]. The resulting two inequivalent types of methyl group occur in the ratio 3:1 and the corresponding tunnelling spectrum shows two tunnelling transitions with this intensity relationship.[69] The ratio of the integrated inelastic and elastic intensities also indicate, in accordance with eq. (6), that no further undetected methyl group excitations are present. In the case of tetramethyl lead[70] the crystal structure is unknown. From the qualitative similarity of the spectrum shown in figure 4 to that of tetramethyl tin, it can be confidently concluded that tetramethyl lead has the same crystal structure. The tunnelling line with the lower intensity shows the larger tunnel splitting and hence has the weaker potential. This means that the molecule is elongated along the threefold axis. The opposite situation occurs for tetramethyl tin, where the compression of the molecule along the threefold axis postulated on the basis of the tunnel spectrum[69] has been confirmed by diffraction measurements.[88] Figure 4 further shows a typical temperature evolution of a tunnelling spectrum, the lines broadening as they shift towards the elastic line (see eq. (17)). In the present case, the regime of jump reorientation, manifested by a purely quasielastic line, is reached at quite a low temperature (~28K) due to the weakness of the rotational potential.

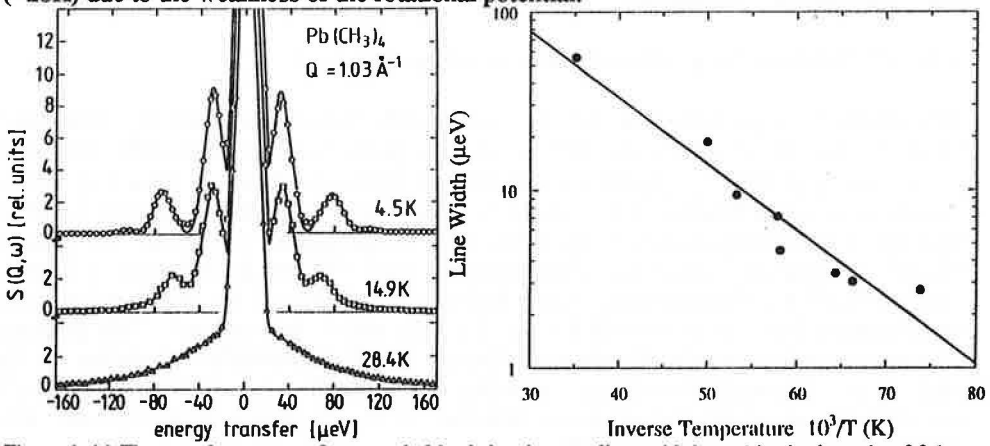

Figure 4. (a) The tunnel spectrum of tetramethyl lead showing two lines with intensities in the ratio of 3:1 as measured on IN5 at ILL with a resolution of 18μeV. Note the rapid spectral change from discrete inelastic lines to a quasielastic feature at a relatively low temperature. (b) An Arrhenius plot of the broadening of the 30.7μeV line with temperature gives an activation energy of 9.0 meV which is identified with a librational mode measured at 9.6 meV.[70]

This example also illustrates some basic problems in deriving accurate rotational potentials in multirotor systems. A determination of the potential up to second order, according to eq. (3), requires that at least two transitions related with a particular rotor are experimentally observed. The E_{01} librational mode can often be determined, but, in the case of tetramethyl lead (and many other compounds), the problem of relating specific tunnelling lines to specific librational modes originating from the inequivalent methyl groups, is encountered. The only experimental possibility of achieving this is by analysing the temperature dependent broadening of the tunnel lines which, according to eq. (17) shows an activation energy $\sim E_{01}$.[9] Spectroscopy can then often identify the librational line and refine its energy. In this manner it has been possible, in the case of tetramethyl lead, to obtain two well-characterised rotational potentials which were capable of estimating consistently the NMR spin-lattice relaxation in the material.

In the present example of tetramethyl lead the different types of methyl group can be identified crystallographically by their unequal occurrence probabilities. On the basis of

the differing intensities of the tunnel lines, the potentials can thus be ascribed to identifiable methyl groups in the crystal unit cell. This is not possible to do experimentally for materials in which no such *unequal* crystallographic distribution exists. The two inequivalent methyl groups in toluene for example have *equal* occurrence probabilities and, in this case, calculations on the basis of pair potentials are the only way to attempt an assignment.

3.1.2. *The hexachloroammonium metallates*

Three-dimensional rotors have a more complex tunnel split librational groundstate than one-dimensional ones. The number of sublevels further depends upon the site symmetry as detailed in refs.[6, 89] The simplest case is realised in systems where the symmetry of the environment is the same as that of the molecule. This situation exists in the case of the hexachloro-ammonium metallates $(NH_4)_2MeCl_6$, where Me is a tetravalent metal ion.[12,89-90] The crystal structure is of the CaF_2 type with space group $Fm3m$ and atomic positions other than that of the Cl^- ion are determined by symmetry. The librational groundstate in this case is a triplet with two allowed transitions. The Pd compound shows the weakest potential and the tunnel spectrum is reproduced in figure 5. The insert shows the level scheme including the total nuclear spin of the states and the allowed transitions.

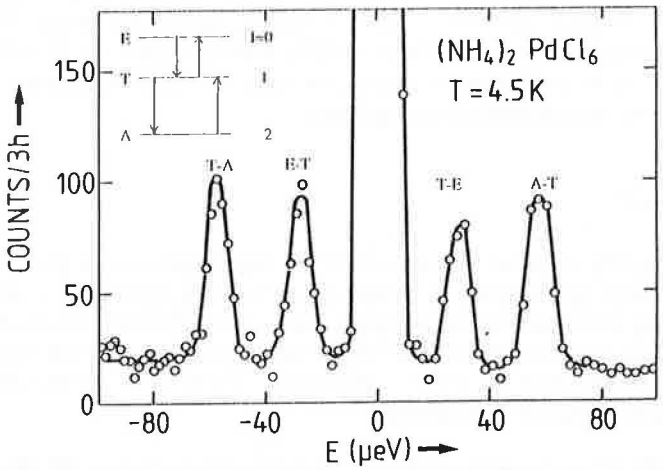

Figure 5. The tunnelling spectrum of the NH_4^+ ion in $(NH_4)_2PdCl_6$ as measured on IN5 with a resolution of 9μeV at a temperature of 4.5K. The insert shows the level scheme of the split groundstate of the 3-dimensional rotor.[12]

Applied pressure reduces the intermolecular distances and thus will increase the rotational potential and reduce the tunnel splitting as shown in figure 6(a). The exponential decrease is due to the increasing pair interaction with decrease in intermolecular distance. From the slope the exponent n^* of the dominant interaction can be extracted as indicated in section 2.1(iii). In materials where the atomic sites are fully determined by symmetry, the change of all interatomic distances can be described by the isothermal compressibility. From eq. (8) we then get an exponent of $n^*=11$. The high value emphasises the importance of steric forces in determining the rotational potential: at orientations between the equilibrium positions (i.e. near the maxima of the potential), the atoms approach each other rather closely and the repulsive part of the Born-Mayer potential dominates.

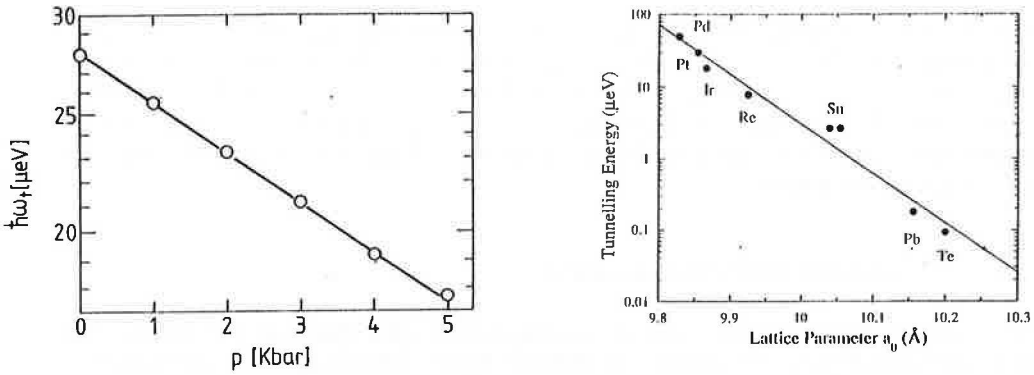

Figure 6. (a) The effect on the E-T transition in $(NH_4)_2PdCl_6$ of applied pressure showing the shift to lower energies.[12] (b) The T-A tunnel frequencies measured at 4.2K as a function of the RT unit cell dimension a_0 of the $(NH_4)_2MeCl_6$ family where *Me* = *Pd, Pt, Ir, Re, Sn. Pb* and *Te*. The shift is opposite to that shown in 6(a).

In contrast, a reduction of tunnel splitting occurs in this family of materials when the *Pd* ion is replaced by *Pt, Ir, Re, Sn, Pb* and *Te* and the lattice parameter increases, as shown in figure 6(b). This behaviour is in contrast to the straightforward explanation of the results from the pressure experiment and has its cause in the influence of the chlorine ions on the ammonium rotational potential. With reducing lattice parameter the chlorine ion approaches a high symmetry position x=0.25. For this value the *Cl* sublattice becomes *fcc*. The transition towards a rotational potential of higher symmetry with decreasing lattice parameter increases the tunnel splitting.

3.1.3. *Disorder*

The extraordinarily sensitive dependence of the tunnel splitting on the rotational potential makes tunnelling spectroscopy a unique probe for any type of disorder. There are a number of very different kinds of disorder, some of which lead to well-characterised new sites, and others which cause a broad distribution of potentials, and hence a broad (and continuous) distribution of tunnel splittings. Even in a chemically pure single-component system we can have disorder.

As an example let us consider methane. At temperatures below 3K the material can be considered as an alloy of molecules in the real *A* groundstate and others in tunnel excited *T* and *E* states. The difference of the wave-functions makes the interaction of these two types of molecule different. The statistical occupation of sites with the two types of molecule, non-excited and excited ones, yields different surroundings with different potentials and explains the finite widths of the tunnel lines.[91] Only at milliKelvin temperatures, and provided that the spin conversion has been accelerated by the addition of paramagnetic oxygen impurities, do the tunnelling lines narrow to match the instrumental resolution. In the case of mixed protonated/deuterated methane at concentrations where the system is close to the transition into phase III, the conversion into the groundstate of CH_4 drives this transition. A sample kept at 3K will take one day, a typical conversion time, to transform into phase III.[28]

Similar variations of the neighbourhood are observed for mixtures of chemically different species: mixed protonated and deuterated compounds,[24,28-29,82] or methane in rare gases at

finite concentrations.[20,92] In the latter case molecular neighbours contribute to the potential, in addition to the crystal field, by their orientation-dependent molecular field. The physics of such mixtures, such as CH_4/Kr[21,92] and Ar/N_2 with CH_4[93] at low temperatures, has been discussed by analogy with magnetic systems as an orientational glass state. A similar mechanism is active in the metal hexammines, for example $Ca(NH_3)_6$.[58,94] It appears that this material is always prepared with small deviations ε from stoichiometry. The empty sites modify the potential of the immediate neighbours and, via orientational relaxation, of the more distant ones also. The broad distribution of observed tunnel frequencies[94] are certainly partly due to this type of disorder, frustration being another cause.

A special type of disorder appears in rare gas solids prepared in non-equilibrium conditions. Due to the very small difference in energy between the equilibrium *fcc* and *hcp* structures, stacking faults with local hexagonal symmetry are created at high concentrations. A molecular probe such as CH_4 is distributed statistically in this matrix. Thus we observe molecules at *fcc* sites with their tunnelling transitions at 0.98 meV (known from samples prepared in thermodynamic equilibrium). Molecules at *hcp* sites are found to show smaller splittings of 0.7 meV for the krypton matrix,[92] in agreement with theoretical models[41] based on fundamental interactions. As seen in figure 7 the lines are strongly broadened due to other types of disorder. The relative intensities of the inelastic lines are a measure of the probability of occurrence of stacking faults in the material. In the case of an argon/methane matrix,[18] the lower energy lines, and hence the *hcp* sites, are observed to disappear with sample annealing.

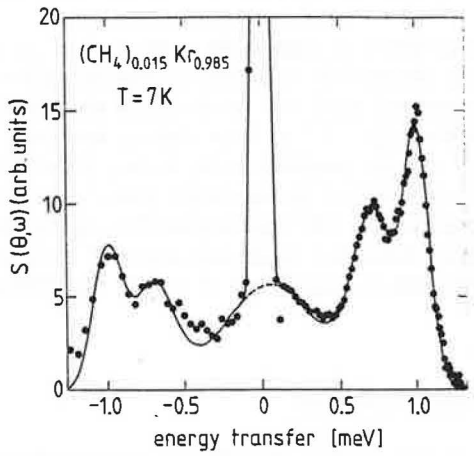

Figure 7. A spectrum of the rotational excitations of CH_4 molecules in a disordered krypton matrix as measured at a temperature of 7K on IN5 with a resolution of 60μeV.[95] The methane concentration was 1.5%. The solid line is a fit to the data.

3.1.4. *Fundamental interactions*

In only a few cases has an attempt been made to understand the rotational potentials on the basis of fundamental interactions. Examples are CH_4,[96-97] nitromethane,[59] p-xylene,[60] and toluene.[60] The necessary calculations require a broader knowledge of the system than just the rotational excitations. Firstly, reliable intermolecular interactions, usually parameterised as transferable pair potentials (PP) according to eq. (11), must be known. Furthermore, the atomic positions at liquid helium temperature, where tunnelling is measured, are needed. Finally, the charges on the atoms enter because of the Coulomb

interaction. These electrostatic terms are nowadays best determined from first principles calculations by using, for example, the molecular orbital program GAUSSIAN90.[98] PP are most well known for pure hydrocarbons and thus the majority of calculations have been done with such compounds.

In the case of toluene the existence of two non-equivalent methyl groups in the low temperature α-phase yields an internal consistency check for the validity of the results. The work[60] concentrates like others on a test of the various PP parameterisations existing in the literature. It shows that neglecting the Coulomb interaction, which used to be done when PP were originally established, yields inconsistent results. The PP of Kitaigorodskii[99] were found to be especially good: calculated tunnel splittings agree with observations within a factor of two. For p-xylene[60] the hydrogen-hydrogen interaction was found to determine the dominant part of the rotational potential while the hydrogen-carbon interaction only contributes ~10%. An improved agreement with experiment was found when the repulsive part of the PP was reduced.

From today's point of view it appears that the early modelling of PP suffered from the problem that part of the electrostatic interaction was incorporated into the PP interaction itself because of an inadequate knowledge of the charge distribution. Today the availability of advanced programs and superior computational power allows much more improved calculations of electron densities in molecules from first principles to be done. Thus the possibility now exists of a new description of intermolecular interactions, pair potential parameters which simultaneously take into account the best calculated charge distributions, and high quality spectroscopic data.

All the work discussed above has been done in the framework of the single particle model. The rotational potentials are obtained by summing up pair interactions of the static lattice, and the energies of the rotational modes in the potential are calculated from the single particle Schrödinger equation (2). It has been shown, however, that both the direct coupling to other rotors,[46] and the coupling to the lattice phonons,[9] rescales the tunnel splittings and librations with respect to the single particle model. Further progress requires the development of theories which go beyond the single particle model towards a unified description of lattice dynamics, molecular quantum rotation and the interaction with phonons. This represents a major field of future theoretical work in rotational tunnelling.

3.1.5. *Ammonia in intercalated graphite*

Small molecules such as hydrogen,[38] methane[39] and ammonia[36-37,40,100-102] will absorb, in an apparently continuous and non-stoichiometric manner, into the large two-dimensional galleries in graphite intercalation compounds. Such galleried structures form a favourable environment in which to study with neutrons the phenomenon of adsorption and adsorption potentials, which are of great interest in the various fields of surface physics such as catalysis, by means of tunnelling spectroscopy. In particular the variation of tunnelling behaviour with adsorbate concentration in caesium graphite turns out to show a surprisingly diverse range of behaviours: hydrogen sits in interstitial sites and exhibits a rich and varying set of tunnel spectra; ammonia shows similar spectral behaviour but is chemically bound to the intercalate; and methane, isoelectronic to ammonia, shows no evidence of tunnelling within the neutron energy range observable, possibly due to a lack of symmetrical registry with the graphite lattice.

Alkali metals *Me* will absorb into graphite, producing complex layered structures, the details of which depend upon the alkali metal concentration, its ionic radius and the

temperature. As the alkali metal concentration increases, the structure passes from dilute higher order *stages* to a second stage compound (so-called because there are two layers of graphite separating each layer of intercalated alkali metal) with a stoichiometry of $C_{28}Me$ and, at the highest concentration, a first stage compound (having one layer of graphite per alkali metal layer) which has a stoichiometry of C_8Me. Absorption of small molecules into second stage intercalation compounds is thermodynamically most favourable, and provides a true two-dimensional space with little direct interlayer interaction between the intercalated alkali metal atoms. At low temperatures the alkali metal lattice registers with the graphite lattice as locally commensurate $\sqrt{7}d$ by $\sqrt{7}d$ islands of alkali metal atoms separated by domain walls or discommensurations, depending on the concentration of alkali metal, as shown in figure 8. The $\sqrt{7}d$ by $\sqrt{7}d$ structure of alkali metal atoms is a hexagonal lattice rotated through 19.1° with respect to the underlying hexagonal graphite structure.

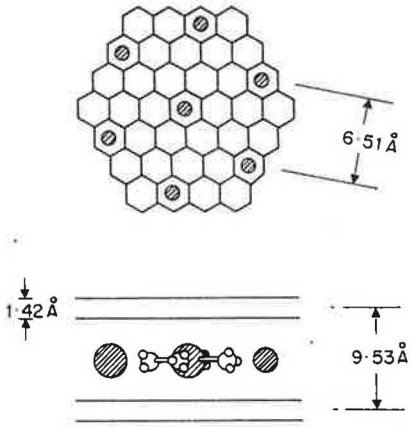

Figure 8. The second stage graphite intercalation compound $C_{28}Cs$ showing the decoration of the lattice with the caesium atoms. A side view gives a representation of a $Cs(NH_3)_4$ molecule following absorption of NH_3 by the intercalate to form $C_{28}Cs(NH_3)_x$.[40]

In the second stage caesium compound methane sits isolated in the triangular sites between three caesium atoms. Ammonia, on the other hand, chemically binds to the caesium atom, in what is thought to be a tetrammine molecule, by analogy with the potassium intercalate[100-102] where a planar and approximately four-fold co-ordination of the ammonias is found. Thermodynamic limits on gas uptake also point to a $Cs(NH_3)_4$ molecule included into the structure and this is consistent with the evolution of the tunnelling spectra with ammonia concentration, and with high resolution neutron diffraction studies. The inelastic spectra out to an energy transfer of 2meV and the diffraction pattern in the region of the *(003)* interplanar reflections were studied simultaneously using the IRIS spectrometer.[37-40] The data are shown in figure 9 as a function of NH_3 concentration up to 1.9 molecules of ammonia per caesium atom. The diffraction patterns show that the extreme range of the intercalate c-axis swelling is 0.44Å but that the absorption process is not continuous as might be inferred from the thermodynamic data. Instead there exist at least two well-defined intermediate phases with distinct c-axis swellings and probably more, and these phases coexist over wide concentration ranges.

The inelastic spectra show a similar variation of distinct features with ammonia concentration and these features can be directly linked to the changes in the structure indicated by the diffraction data. At low concentrations a 126 μeV tunnel line and a 640 μeV almost-free rotor line of equal intensities are observed, pointing to an equal number of free rotors and tunnelling rotors per caesium atom. The intensities of these lines have a

similar variation with concentration, disappearing at $NH_3/Cs>1.25$, the same concentration at which the 0.24Å swollen *(003)* diffraction line disappears. At concentrations of 0.74 and higher, a second tunnel line at 89 μeV becomes the dominant inelastic feature, again echoing similar changes in the diffraction pattern. The temperature dependence of the 89 μeV and the 126 μeV lines shows interestingly different behaviour indicating a distinctly opposing coupling mechanism to lattice phonons. The 89 μeV line falls in energy with temperature, whereas the 126 μeV line rises dramatically as shown in figure 10.

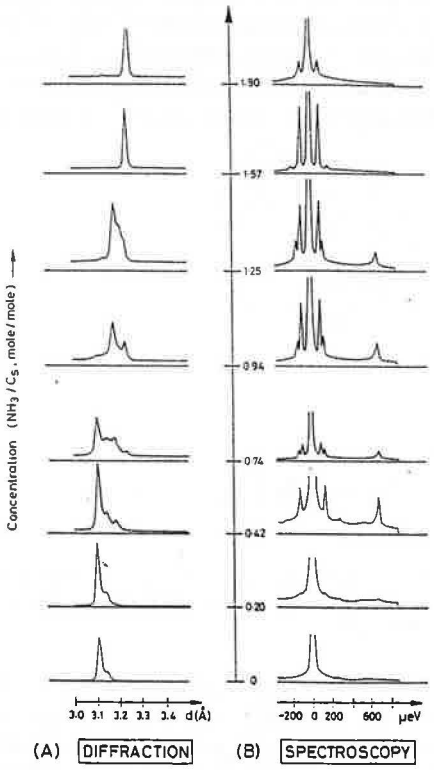

Figure 9. Simultaneous diffraction patterns around the *(003)* reflection, and tunnelling spectra from $C_{28}Cs(NH_3)_x$ as a function of NH_3 concentration x showing the parallel evolution of structural and dynamic features.[40]

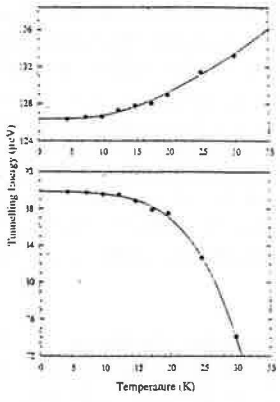

Figure 10. The opposing shifts with temperature of the 89μeV and the 126μeV tunnelling lines in $C_{28}Cs(NH_3)_{1.25}$.[40]

More recent measurements at higher concentrations and higher resolution[103] show conclusively that a third tunnel line, suggested in the lower resolution data, does in fact appear for $NH_3/Cs = 1.90$ at an energy of 26.3 μeV, initially together with the 89 μeV line and, as NH_3/Cs rises above 2.0, it becomes dominant. As the thermodynamic concentration limit is approached ($NH_3/Cs \sim 2.3$) a fourth tunnel line appears at ~16 μeV. Intriguingly, at these higher concentrations, the diffraction lines, in contrast to the tunnel lines, appear to indicate a smooth shift to larger swellings, but this may be an artefact due to resolution limits and disorder effects in the sample. The conclusion that there is a direct link between the structural evolution of the absorption process and the dynamical behaviour of the NH_3 groups is clear. These changes are partly due to step changes in the orientation of the assumed $Cs(NH_3)_4$ molecular unit within an intercalate layer, partly to the production of a concentration-modulated ternary intercalate, with some caesium layers filled and some empty and, at high concentrations, to the effect of intermolecular interactions.

3.1.6. *The Q-dependence of excitations in methane*

Solid methane has attracted considerable theoretical and experimental investigation because of its apparent simplicity. Below its freezing point CH_4 remains in an orientationally disordered plastic phase down to 20.4K where it undergoes a phase transition to the partially ordered structure of CH_4-*II*. Three of the four methane molecules in the *fcc* unit cell are orientationally ordered, librating about the minima of a strongly anisotropic potential, whereas the fourth molecule is disordered and rotates freely. Direct evidence that the structure of solid CH_4 is the same as that of CD_4 does not exist, because the strong incoherent scattering from the protons precludes accurate neutron diffraction measurements, although this has been intuitively assumed in spectroscopic investigations. Since the dynamical behaviour of methane is strongly related to the structure of its solid phases, important structural information can be deduced from incoherent inelastic neutron scattering.

The original model of James & Keenan,[104] which treated the methane molecules as pure octopoles, was extended by including higher order multipole moments together with a *Lennard-Jones* contribution to the interaction potential.[97] The orientational potential can be expressed according to eq. (13) as the sum of a weak crystalline field of cubic symmetry V_C and a strong molecular field W, where ω represents the Euler angles of the molecules

$$V(\omega_i) = V_c(\omega_i) + W(\omega_i, \{\omega_j\}) \quad . \tag{20}$$

The crystalline field V_C is a single particle potential, depending only on the orientation of the molecule i. It is present at all molecular sites. The molecular field is essentially determined by the octopole-octopole interaction. Such interactions acting on a methane molecule surrounded by 12 orientationally ordered neighbours cancel for symmetry reasons, leading to a vanishing molecular field related to the free rotor transitions. The ordered methane molecules show a tunnel split librational groundstate similar to that shown in figure 5 for $(NH_4)_2PdCl_6$. The first excited librational multiplet occurs above 6meV. The energy level schemes have been calculated on the basis of empirical atom-atom potentials.

In figure 11 the spectra from CH_4-*II* very clearly reflect the two different kinds of rotational excitations.[105] The mode at 1.07meV represents the 0-1 transition of the

disordered molecules. The energy of this transition is 18% lower than that expected from a completely free methane molecule. The two peaks at lower energy transfers, 75μeV and 145μeV, represent the tunnelling transitions *T-E* and *A-T*. *A-E* is not allowed for reasons of nuclear spin conservation. At higher momentum transfers, the *0-2* and *0-3* transitions of the disordered molecules are observed at 2.9meV and 3.2meV, considerably closer than would be expected from the theoretical level scheme.

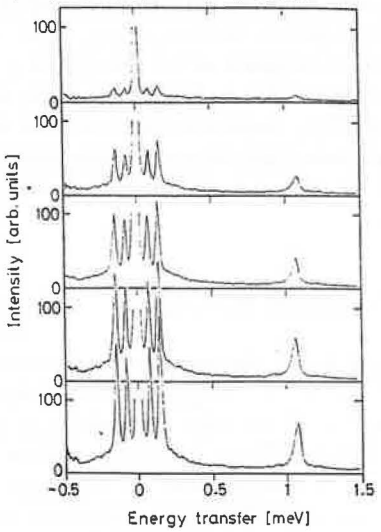

Figure 11. The two tunnelling transitions at 75μeV (T-E) and 145μeV (A-T), together with the free rotor line at 1.07meV, in phase-II of solid methane as measured at 5K on IRIS at momentum transfers Q from 0.3 to 1.7 Å^{-1}.[105] The instrumental resolution was 15μeV.

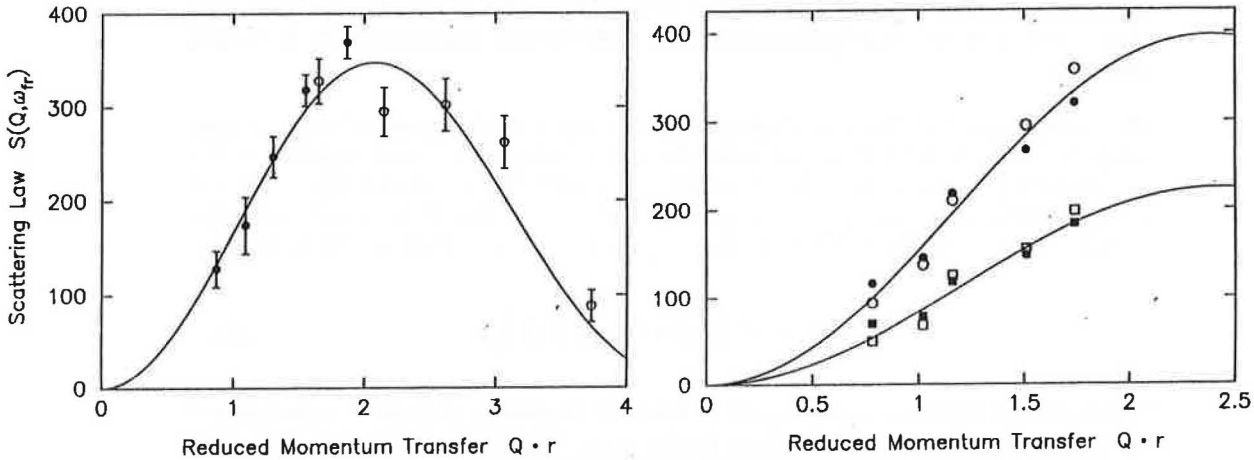

Figure 12. The integrated intensities of the excitations in phase-II of solid methane shown in figure 11 as a function of $Q.r$, the reduced momentum transfer, where r is the radius of gyration of the molecule. (a) refers to the free rotor line and (b) refers to the T-E (circles) and the A-T (squares) tunnelling transitions respectively.[105] The lines are a fit of the Extended James-Keenan model for *CH_4-II*.

Additional information is contained in the scattered intensities which are closely related to the wave-function of the scatterer. A comparison of the Q-dependence of the intensities with theoretical predictions by Ozaki[96] is shown in figure 12 for the almost-free rotor line and the two tunnelling lines.[105] The extended wavefunctions lead to a strong decrease of intensity with Q. The effect is similar to that of a Debye-Waller factor multiplying the structure factor of δ-localised protons.[74] The only free parameters in the fit were the

intensities of the free rotor line and the tunnelling transitions. The ratio of the two intensities was determined to be 3.04 ± 0.05, thus providing the first direct experimental evidence for the 3:1 ratio of the number of orientationally ordered and orientationally disordered molecules in CH_4-*II*.

3.1.7. *Excitations in 4-methyl pyridine*

The first sample in which quantum excitations of methyl groups were observed with neutron spectroscopy was 4-methyl pyridine, $C_5NH_4.CH_3$, in 1975.[1] Since then it has been examined regularly with increasingly high resolution,[24,47,106-110] often being the source of surprising new results which have challenged the accepted views of the interpretation of quantum motions. Since the methyl group in 4-methyl pyridine is linked to an aromatic pyridine ring, the potential barrier for internal rotation is extremely low for the isolated molecule, and remains so even in the solid. The compound has been investigated by numerous different techniques and yet the potential function governing the methyl torsion remains a subject of discussion.
The first study using neutrons[1] revealed an intense line at 520μeV and two weaker lines at higher energies. From the relationship between the energies of the lines, the spectrum was interpreted as being due to hindered rotation or tunnelling of the CH_3 group in a sixfold potential. A frequency ratio of ~5 of the hindered rotations in the protonated and deuterated compounds[106] is consistent with tunnelling in either a threefold or a sixfold potential. Later results[107] claimed that the potential was in fact threefold and observed[47] that the line at 520 μeV was in fact a triplet, comprising two weaker lines at 468 μeV and 535 μeV, on either side of a strong line at 510 μeV as shown in figure 13(a).

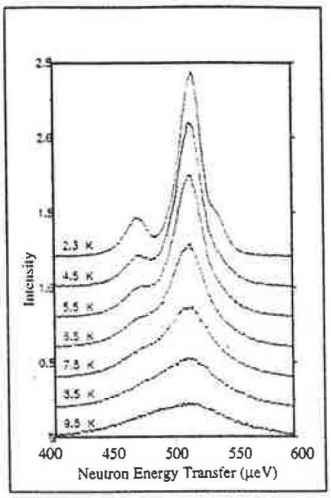

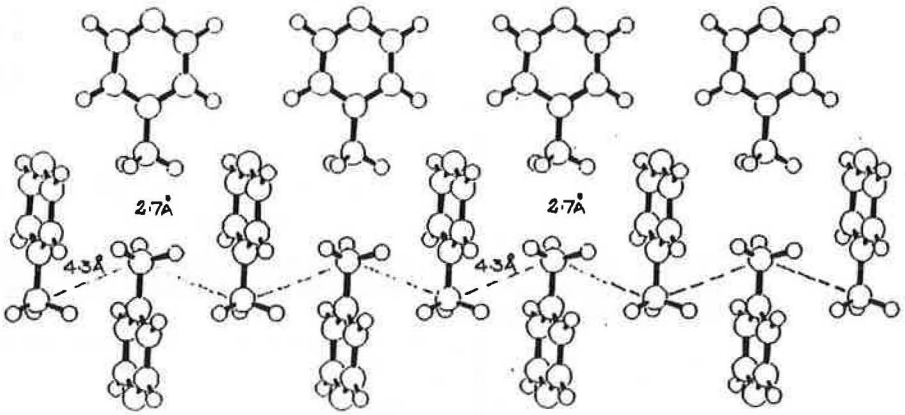

Figure 13. (a) The excitation observed in 4-methyl pyridine on IRIS as a function of temperature showing, in the 2.3K spectrum, the triplet structure of the band.[47] (b) A cut through the *c*-*a* and *c*-*b* crystallographic planes showing the 1-dimensional zig-zag chains of CH_3 groups along the *a* and *b* axes, and the closeness of the CH_3 pairs along the *c* axis.[24]

The crystal structure of 4-methyl pyridine at 4 K is tetragonal, $I4_1/a$, with four equivalent molecules in the unit cell.[111] The dominant dipole-dipole interaction leads to an antiparallel ordering of the molecules along the c-axis with methyl groups facing each other. Each methyl group is part of a linear chain zig-zagging along the crystallographic *a* and *b* axes at different heights up the long tetragonal axis as shown in figure 13(b). Suggesting that the opposing CH_3 groups were dynamically coupled, an extension to the

Hamiltonian, given in eq. (16), was proposed[47] which was able to explain the frequencies of the triplet line.

In an attempt to determine whether the three components in the spectrum are due to intermolecular or intramolecular effects, a series of measurements were made at 2K of a range of dilutions of fully protonated material with the perdeuterated compound[24,104] which showed a continuous shift of the main peak to lower energies with increasing dilution, indicating the existence of collective motions of the methyl groups. At the lowest dilution the main peak appears at ~360μeV, a shift of one-third, and as the temperature is raised to 15K the peak position also rises to regain the ~520μeV value of the pure hydrogenated compound, as shown in figure 14. A totally new interpretation,[24] expressed in terms of breather modes within the framework of the quantum sine-Gordon theory as given in eq. (15), and applied to the two sets of one-dimensional chains of methyl groups in the crystal structure, has been proposed to explain these data. Since the change of CH_3 group orientation from neighbour to neighbour is small, the coupling term in eq. (15) has been linearised and the resulting expression is equivalent to that of the sine-Gordon theory. The solutions of the equation include solitons, phonons and breathers (bound soliton-antisoliton pairs), which propagate along the infinite chains. The triplet excitation is then explained as two weak coherent tunnelling lines, at 468 μeV and 535 μeV centred on the breather mode at 510 μeV.

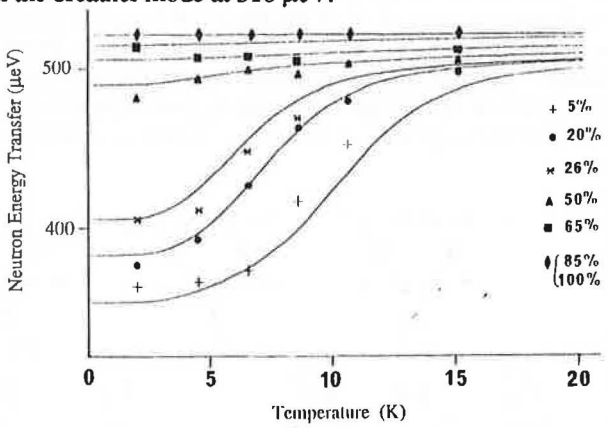

Figure 14. The experimental frequencies of the breather mode in isotopic molecular mixtures of h_7 and d_7 4-methyl pyridine at a series of h_7 concentrations from 5% to 100%. The lines are the calculated values from the quantum sine-Gordon theory.[24]

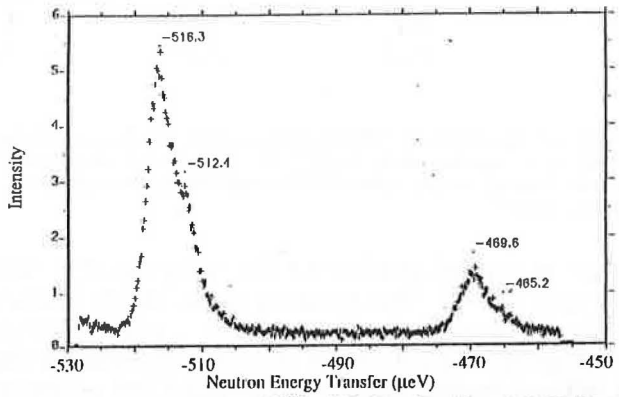

Figure 15. A high resolution spectrum, taken at 1.5K, of the breather line at 516μeV, and the lower energy coherent tunnelling line at 470μeV, in 4-methyl pyridine, as measured using the temperature scanning offset monochromator on IN10 with a resolution of ~ 2μeV. A partially resolved line is visible at 512μeV.[110, 115]

As the protonated material is diluted by deuterated material, the infinite chains of CH_3 groups are reduced in length by the presence of CD_3 groups, which act as reflective walls for the breather which becomes trapped in a finite length chain and its energy falls progressively with dilution. The quantum sine-Gordon theory is able to explain all the features of the unusual dynamics of 4-methyl pyridine, including later measurements from samples with partially deuterated methyl groups,[109] and very high resolution measurements from the purely hydrogenous compound,[110] where the excitations of different chain lengths are able to be partially resolved, as shown in figure 15.

The application of the pocket state formalism[45] to a coupled linear chain of four methyl groups would require a different interpretation of the spectra but it yields only a single tunnelling line.

3.2. *Experimental techniques*

3.2.1. *Selective deuteration*

Because the neutron carries a spin of 1/2, when it scatters from a hydrogen nucleus, also spin 1/2, the interaction can be either in the parallel or antiparallel configuration. The scattering lengths of these two interactions differ greatly and it is this difference which generates the unusually high 80 barns incoherent cross-section of hydrogen. The neutron is therefore extremely sensitive to hydrogen atoms in a material. For a sample containing a single isotope with non-zero nuclear spin two-thirds of the incoherent scattering is spin-flip and one-third is non-spin-flip. Coherent scattering is totally non-spin-flip. Transitions between tunnelling states necessarily involve a spin flip of the tunnelling atomic nucleus and consequently it can only be detected by incoherent scattering. Deuterium, whose nucleus carries a spin of one, has a low incoherent cross section (2.05 barns) and a relatively high coherent cross section (5.59 barns). The neutron is therefore 40 times less sensitive to deuterium tunnelling than to hydrogen tunnelling.

Deuteration of a proportion of the protonated molecules in a sample, or of a number of the hydrogen atoms on the tunnelling rotor itself, or of the non-tunnelling hydrogen atoms on the molecule under study can therefore serve a number of useful purposes in enabling the dynamics of the rotor under investigation to be understood. In the first case, direct coupling between rotors can be investigated as has been done for lithium acetate[25] and 4-methyl pyridine.[24] In the second case the change of dynamics of the rotor when its symmetry is changed by the substitution of a mass 2 atom for a mass 1 atom can be exploited to advantage as in the case of methane on the surface of graphite[33] and again 4-methyl pyridine.[109] Partial deuteration of one-dimensional rotors suppresses the tunnel motion due to the symmetry reduction of the rotor. Only in the limit of free rotation is quantum motion still observed. In the third case, if the hydrogen atoms on a tunnelling rotor represent only a small proportion of the total hydrogen atoms in the sample itself, the background scattering can be significantly reduced by deuterating these non-tunnelling protons, particularly when the tunnelling line is very close to the elastic line.

Deuteration in this manner is of course a specialised and expensive chemical preparation process. However, when included in with the cost of generation of the neutron beam and provision of other ancillary equipment such as liquid helium cryostats, it can be a relatively minor contribution to the overall resources consumed by an experiment and yet can enhance the outcome greatly.

3.2.2. *Sample preparation and sample environments*

Samples must not be so thick that multiple scattering becomes a problem. This depends upon the application. If the position of tunnelling peaks is all that is required, a sample which scatters 30% of the beam can be tolerated. If relative intensities of lines in a multi-line spectrum are required, or if the variation of intensity with momentum transfer Q is needed the sample should not scatter more than 10% of the incident beam. In practice, for a standard organic material, this means a sample thickness around 2mm for 30% scattering and about 0.5 mm for 10% scattering. The sample is normally slab-shaped, but if Q-variation is being investigated, a hollow cylindrical sample-holder has many advantages.

Samples can be studied under pressures ranging from ambient to around 25 kbars, in practice. Pressure cells up to 4 kbars using helium as the pressure transmitting medium have sample volumes of 2 to 3 cm^3. The sample should preferably be diluted with aluminium powder, since it would otherwise be too thick. The pressure in these cells can be varied *in situ* which make it convenient as a thermodynamic variable. For higher pressures more massive cells must be used in which the sample volume is significantly smaller (ca. 350mm^3) and the cell must be removed from the cryostat each time that the pressure has to be changed. Run times can often be up to 24 hours in these cases. The pressure is applied to the sample by mechanical means - pistons or anvils - and if the pressure is to be applied hydrostatically a pressure transmitting medium, often carbon disulphide, must be mixed with the sample.

Gases such as methane and ammonia can be applied in situ to samples such as intercalates[36-40,100-103] and onto surfaces such as Grafoil[112-114] via capillaries in the cryostat in order to study these materials, which can only be prepared uniquely. In these cases it is advantageous to have a measure of the diffraction pattern simultaneously, to follow any structural evolution and check the lattice parameters. When a study of condensed gases and their mixtures is required, such as that carried out very effectively and systematically for of the methane/rare gas systems,[20-21, 91-92, 95] it is often necessary to solidify the pure or mixed gases inside the sample holder directly. In these cases the sample holder is kept cold in the cryostat whilst the capillary leading to it is heated to avoid solidification prior to the gases entering the sample holder. This technique has been used successfully for the matrix isolation of small molecular materials such as tetramethyl tin in an argon matrix. This field has been surveyed quite recently by Langel.[15]

Tunnelling is a quantum mechanical process which requires low temperatures for its observation. Normally the temperatures attainable with a pumped helium cryostat (~1.2K) are quite acceptable, but in certain cases advantage can be obtained by the use of dilution fridges which take the sample temperature down to around 30mK. This is not routinely necessary since phonons only induce transitions to excited librational levels consisting of the same symmetry. Transitions within the tunnel-split ground-state $\hbar\omega_t$, because they involve a change of spin, cannot be mediated by phonons. Thus the sample temperature must fulfil the condition that $T \ll E_{01}$ but not that $T \ll \hbar\omega_t$. This latter condition is, however, required in translational tunnelling where spin and space wavefunctions are not correlated.

3.2.3. *Spectrometers*

We can define a rule of thumb for the dynamical range required of a spectrometer for tunnelling spectroscopy by considering the range of excitations exhibited by typical samples.

The lowest energy free-rotor transition in one-dimensional rotors occurs at an energy transfer of B as defined in eq. (1). Any non-zero potential will reduce the energy of this transition. In the case of methyl groups B=655μeV and for ammonia B=782μeV. Potentials of amplitude ~50meV will reduce the tunnel splitting to ~1μeV, which represents the lower experimental limit for detection at present. The lowest free-rotor transition of three-dimensional spherical tops is $2B$. Thus for methane the free rotor limit is about 1.31 meV. Hydrogen is the molecule with the largest value of B, being 7.3 meV. Tunnelling transitions of H_2 in restricted environments such as intercalates, however, appear at energy transfers which are much lower.[14,38,114] This then determines the dynamic range of spectrometers required for experimental investigations: an energy transfer range from 0.5μeV to a few meV.

Tunnelling lines at the lowest temperatures are very narrow, indeed they are one of the only ways which can be used to determine the inelastic resolution of a spectrometer. Line broadenings of the order of the tunnel splitting occur as the temperature of the sample is raised from the base temperature to a temperature somewhere between 15 and 50K. The lines will be strongly broadened and shifted such that they merge into either the background or the elastic line, depending on the sample. Therefore we require spectrometers which have resolutions in the μeV range: less than 0.3μeV is presently not attainable and greater than 250μeV is too broad for these purposes.

In order to attain these kinds of absolute energy resolutions we must utilise the slowest neutrons, always bearing in mind that as Q becomes small the intensity of tunnelling transitions becomes quite weak, following the structure factors given in eq. (6) and therefore the neutron energy must not be too small. Accordingly the majority of instruments which are used for tunnelling spectroscopy have been built on beamlines which view cold moderators where the flux of low energy, long wavelength neutrons is considerably enhanced. There are two distinct kinds of spectrometer which are used in these studies, both of which utilise neutron time-of-flight as an energy selector. These are the direct geometry spectrometers (such as IN5 at ILL and MIBEMOL at LLB, Saclay, which utilise a monochromatic incident beam) and the indirect, or inverse, geometry spectrometers (such as IN10 and IN13 at ILL, IRIS at ISIS, LAM80 at KENS, Tsukuba and the new backscattering spectrometer at Jülich) all of which utilise large area crystal analysers after the sample.

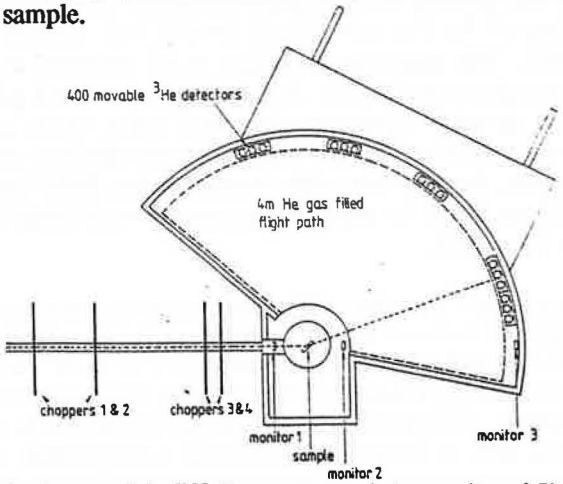

Figure 16. A schematic diagram of the IN5 direct geometry 4 chopper time of flight spectrometer at ILL, showing the array of detectors at 4 metres from the sample position.[3]

Looking at the direct geometry spectrometer first, let us examine the design of IN5[3] at the ILL High Flux Reactor. The instrument is illustrated in figure 16. Four phased disc choppers monochromate and pulse the neutron beam which is incident upon the sample, and the spectrum of scattered neutrons is measured by time of flight analysis over a 4-metre flight path to a large array of helium-3 detectors set on the arc of a circle.

Scattering angles from 5° to 130° can be covered simultaneously and the total detected solid angle subtended is ~0.65 steradians. The elastic peak to flat background ratio exceeds 2500:1. Each chopper has an aperture which is equal to the width of the incident neutron guide. The transmission function of each chopper is therefore triangular, which gives IN5 one of its most powerful properties - a triangular resolution function, unique amongst neutron spectrometers. The incident monochromatic neutron energy can be varied continuously between 0.3meV and 5meV by a computer-controlled rephasing of the choppers, providing energy resolutions at the elastic line of between 3.2μeV and 200μeV. The highest resolution is achieved using 16.5Å wavelength neutrons. The energy transfer range can therefore be matched to the problem under investigation. MIBEMOL at LLB Saclay is an IN5-type machine but has six phased choppers instead of four, two pairs of which are counter-rotating. At least three machines of similar design are under construction world-wide, at HMI Berlin, PSI Zurich, and NIST Washington.

Following on to indirect geometry instruments, let us examine the design of IRIS[4] at the ISIS pulsed source. The spectrometer is illustrated in figure 17. It consists of a long incident flight path from the liquid hydrogen moderator which delivers a white pulsed neutron beam through a neutron guide to the sample sitting at 36.5 metres from the source. This flight path serves to time-sort the neutron beam such that the incident neutron energy can be measured with microelectronvolt precision by time-of-flight. The neutrons scattered from the sample are analysed by a large array of single crystals which serves to reflect a single scattered neutron energy back to an array of scintillator detectors situated close to backscattering geometry (θ_B=87.5°) in order to match the resolution of the primary spectrometer. Detector angles from 15° to 165° are continuously covered. The analysers subtend ~0.7 steradians. IRIS has two sets of analysers, pyrolytic graphite, and muscovite mica. The graphite analysers have been cooled to 25K which reduces the thermal diffuse scattering background from the analyser by a factor of 12 and provides an elastic peak to flat background ratio of ~ 1250:1. The energy range and resolution δE can be changed in steps by choosing the appropriate diffraction order of the analyser crystals: one obtains δE =50μeV for *PG 004*, 15μeV for *PG 002*, 4.5μeV for mica *004* and 1.1μeV for mica *002*. This latter option utilises 19.8Å neutrons, and a spectrum from nitromethane has been shown in figure 3. An advantage of inverted geometry instruments on pulsed sources is the wide energy transfer range which can be accessed in neutron energy loss with good resolution. Equally important is the ability to measure diffraction patterns simultaneously, thanks to the white incident beam. IRIS has such a diffraction detector array situated at $2\theta_B$=170° which gives a resolution of $\Delta d/d=2.5\ 10^{-3}$ over the d-spacing range from 2Å to 13Å.

The IN10 spectrometer at ILL is also an inverted geometry instrument which uses very large silicon analysers (several square metres) covering ~4 steradians in exact backscattering geometry, and provides resolutions of 0.3 to 1μeV. In the standard set-up of the instrument, the energy variation in the incident beam is provided by a Doppler shifting monochromator. This provides a total energy transfer range of 30μeV normally centred on the elastic line. A recent innovation uses a temperature scanning *NaCl 200* monochromator to generate an energy transfer window 65μeV wide offset from the elastic line by ~500μeV with a resolution of ~2μeV.[115] A spectrum of the breather mode in 4-methyl pyridine[110] measured with this new set-up is shown in figure 15.

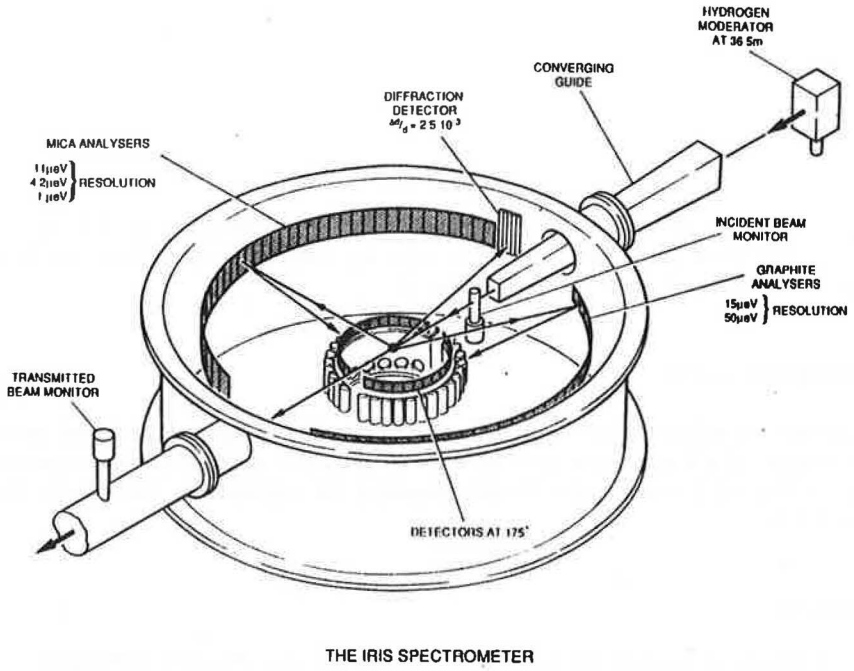

Figure 17. An isometric view of the IRIS time of flight inverted geometry crystal analyser spectrometer at ISIS, showing the two sets of analysers and detectors and the diffraction detector at high angles.[4]

4. Conclusions

Tunnelling rotors show fundamental quantum-mechanical properties in a uniquely simple manner. As such they represent a textbook example of quantum mechanics. The following topics illustrate these properties:

(i) The evolution of the free rotor spectrum from spherical top, to symmetric top, to asymmetric top (e.g. CH_4/Ar).
(ii) The transition from quantum-mechanical motion to classical motion as the temperature rises. In the case of CH_3 groups the quantum mechanical side of the problem has just one degree of freedom and could, in an exemplary manner, document the validity of the correspondence principle.
(iii) Systems can be chosen with an increasing number of interacting quantum particles. This has already stimulated a related evolution of methods in theoretical solid state physics and promises further progress towards solving the problem of large arrays of coupled quantum rotors.

In the field of applications, tunnelling spectroscopy is becoming a standard method like other spectroscopic techniques, for the following reasons.

(i) The spectra contain important structural information.
(ii) The exponential dependence of the quantum rotor transitions on the potential make tunnelling spectroscopy more sensitive to changes in the environment than other methods.
(iii) It provides a new method of access to intermolecular potentials.
(iv) Tunnelling spectroscopy has found, and is continuing to find, application to a wide range of materials, both simple and complex, which are contained in an equally wide range of molecular and crystal environments.

At the time of writing, a number of good quality spectrometers are newly operational or on the point of becoming operational at medium flux neutron sources in Europe and overseas, and the ILL is mid-way through a four-year major refurbishment. The quest for higher instrumental resolutions, the search for new theoretical approaches driven by recent

findings, the expanding range of materials under study, and the promise of future pulsed source developments, will all combine to take the subject of tunnelling spectroscopy through to the 21st century with renewed vigour.

Acknowledgements

It is a pleasure to acknowledge the contribution of all our colleagues to the work presented in this review, which has necessarily been rather selective, particularly the experimental examples. We are grateful to Dr Bernd Asmussen for contributing the information for section 3.1.6.

References

1. B Alefeld, A Kollmar and B A Dasannacharya, J. Chem. Phys **63** (1975) 4415
2. W Press and A Kollmar, Solid State Commun. **17** (1975) 405
3. H Blank and B Maier, *Guide to Neutron Research Facilities at the ILL*, ILL Scientific Secretariat (1988)
4. C J Carlile and M A Adams, Physica B **182** (1992) 431
5. S Ikeda, ed. *Proceedings of Tunnel 902*, KEK report 90-17, 1990
6. W Press, *Single Particle Rotations in Molecular Crystals*, Springer Tracts in Modern Physics, **92** (Springer, Berlin, 1981)
7. A Heidemann, A Magerl, M Prager, D Richter and T Springer, eds. *Quantum Aspects of Molecular Motions in Solids*, Springer Proceedings in Physics, **17** (Springer, Berlin, 1987)
8. W Häusler and A Hüller, Z. Phys. **B59** (1985) 177
9. A C Hewson, J. Phys. C **15** (1982) 3841 & 3855
10. S Clough, A Heidemann, M Paley and C Vettier, J. Phys. C **12** (1979) L781
11. M Prager, W Press, A Heidemann and C Vettier, J. Chem. Phys. **77** (1982) 2577
12. M Prager, W Press, A Heidemann and C Vettier, J. Chem. Phys. **80** (1984) 2777
13. M Prager and A Heidemann, ILL Report 87PR15T(1987)
14. J Eckert, Spectrochimica Acta **48A** (1992) 363
15. W Langel, Spectrochimica Acta **48A** (1992) 405
16. A J Horsewill, Spectrochimica Acta **48A** (1992) 379
17. Y Kataoka, W Press, U Buchenau and H Spitzer, *Neutron Inelastic Scattering 1977* **1** 311 (IAEA, Vienna, 1978)
18. M Prager and W Langel, J. Chem. Phys. **88** (1988) 7995
19. M Prager and C J Carlile, Chem. Phys. Lett. **173** (1990) 524
20. B Asmussen, P Gerlach, W Press, M Prager and H Blank, J. Chem. Phys. **90** (1989) 400, & M Prager, B Asmussen, W Press, H Blank and C J Carlile, J. Chem. Phys. **95** (1991) 569
21. B Asmussen, W Press, M Prager and H Blank, J. Chem. Phys. **98** (1993) 158
22. C Bostoen, G Coddens and W Wegener, J. Chem. Phys. **91** (1989) 6337
23. R Mukhopadhyay, J Tomkinson and C J Carlile, Europhys. Letts.**17** (1992) 201
24. F Fillaux and C J Carlile, Phys. Rev. **B42** (1990) 5990
25. A Heidemann, H Friedrich, E Günther and W Häusler, Z. Phys. B **76** (1989) 335
26. J Stanislawski, M Prager and W Häusler, Physica B **156** (1989) 356
27. Da Zhang, M Prager and A Weiss, J. Chem. Phys. **94** (1991) 1765
28. M Prager and W Press, J. Chem. Phys. **92** (1990) 5517
29. D Cavagnat, S F Trevino and A Magerl, J. Phys. Condens. Mat. **1** (1989) 10047
30. W Wegener, C Bostoen and G Coddens, J. Phys. Condens. Mat. **2** (1990) 3177
31. R Caciuffo, O Francescangeli, S Melone, M Prager, F Uggozoli, G Amoretti, G Coddens and H Blank, Physica B **180 & 181** (1992) 691
32. R P Hughes, M V Smalley, T Rayment and R K Thomas, Can. J. Chem. **66** (1987) 557
33. G Bomchil, A Hüller, T Rayment, S J Roser, M V Smalley, R K Thomas and J W White, Phil. Trans. Roy. Soc. B **290** (1980) 537

34. S Nozé, Y Ozaki, K Maki and Y Kataoka, Int. J. Quantum Chem. **18** (1980) 641
35. J Z Larese, J M Hastings, L Passell, D Smith and D Richter, J. Chem. Phys. **95** (1991) 6997
36. H Zabel et al., in: *Proc. Materials Research Society, Boston, 1988*, & H Zabel, A Magerl and D A Neumann, ILL Experimental Report 9-06-572 (1989)
37. C J Carlile, I McL Jamie, J W White, M Prager and W Stead, J Chem. Soc. Faraday Trans. **87**(1) (1991) 73
38. I P Jackson and J W White, Chem. Phys. Lett. **134** (1987) 397
39. F Trouw and J W White, J. Chem. Soc. Faraday Trans. 2, **84** (1988) 791, 813, 841 & 861
40. C J Carlile, I McL Jamie, G Lockhart and J W White, Mol. Phys. **76** (1992) 173
41. Y Ozaki, J. Phys. Soc. Japan **59** (1990) 1277
42. A Würger, Z. Phys. B **70** (1988) 193
43. I Jencic, J Peternelj, B Cvikl and M M Pintar, Z. Phys. B Condens. Mat. **79** (1990) 251
44. A Würger, J. Phys. Condens. Mat. **2** (1990) 2411
45. W Häusler, J. Phys. Condens. Mat. to be published
46. G Voll, Z. Phys. B to be published (1993)
47. C J Carlile, S Clough, A J Horsewill and A Smith, Chem. Phys. **134** (1989) 437
48. H Blank and G J Kearley, J. Chem. Phys. **87** (1987) 6809
49. A Heidemann, ibid. ref. 7, p 44
50. W Häusler, *Zur Temperaturabhängigkeit des Rotationstunnelns*, PTB-Bericht PG-3, ISBN 3-89429-002-1 (1990)
51. A Würger, Z. Phys. B **76** (1989) 65, & A Würger and A Hüller, Z. Phys. B **78** (1990) 479
52. A Hüller and L Baetz, Z. Phys. B **72** (1988) 47
53. A Hüller, Z. Phys. B **78** (1990) 125
54. A Heidemann, M Prager and M Monkenbusch, Z. Phys. B **76** (1989) 25
55. A Würger and A Heidemann, Z. Phys. B **80** (1990) 113
56. S Clough and A Heidemann, J. Phys. C **12** (1979) 761
57. M Prager, Can. J. Phys. **66** (1988) 570
58. P Damay, F Leclerq, A J Dianoux and W Press, *Springer Proceedings in Physics*. **37**, p.226 eds. D Richter, A J Dianoux, W Petry and J Teixeira (Springer, Berlin, 1989)
59. D Cavagnat and M Pesquer, J. Phys. Chem. **90** (1986) 3289
60. M Prager, W I F David and R M Ibberson, J. Chem. Phys. **95** (1991) 2473, & M Prager, M Monkenbusch, R M Ibberson, W I F David and D Cavagnat, J. Chem. Phys. to be published (1993)
61. A J Nijman and A J Berlinsky, Phys. Rev. Lett. **38** (1977) 408 & Can. J. Phys. **58** (1980) 1049
62. W Häusler, Z. Phys. B **81** (1990) 265
63. A Würger, Z. Phys. B **81** (1990) 273
64. S Grieger, H Friedrich, B Asmussen, K Guckelsberger, D Nettling, W Press & R Scherm, Z. Phys. Condens. Mat. **87** (1992) 203
65. K Guckelsberger, H Friedrich and R Scherm, Z Phys B Condens. Mat. to be published (1993)
66. G J Kearley, H Blank and J K Cockcroft, J. Chem. Phys. **86** (1987) 5989, & ibid. ref 7 p.58 & p.62
67. G Voll and A Hüller, Can. J. Chem. **66** (1988) 925
68. Y Ozaki, J. Phys. Soc. Japan **61** (1992) 1823
69. M Prager, K H Duprée and W Müller-Warmuth, Z. Phys. B **51** (1983) 309
70. M Prager and W Müller-Warmuth Z. Naturforsch. **39a** (1984) 1187
71. S Clough, A Heidemann, A J Horsewill, J D Lewis and M N J Paley, J. Phys. C **15** (1981) 2495
72. Da Zhang, M Prager, Shi-Qi Dou and A Weiss, Z. Naturforsch. **44a** (1988) 151
73. A Heidemann, I S Anderson, B Jeffryes and B Alefeld, Z. Phys. B **49** (1982) 123
74. A Heidemann, I S Anderson, M Prager and W Press, Z. Phys. B **51** (1983) 319
75. M Prager and W Langel, J. Chem. Phys. **85** (1986) 5279
76. A J Horsewill, R M Green and A M Alsanoosi, ibid. ref. 7. p. 2
77. D Cavagnat, A Magerl, C Vettier and S Clough, J. Phys. C **19** (1986) 6665

78. M Prager, C Vettier and S Mahling-Ennanoui, Z. Phys. B **75** (1989) 217
79. A Heidemann, J Eckert, L Passell and W Häusler, Z. Phys. B **66** (1987) 75
80. D Cavagnat, A Magerl, C Vettier, I S Anderson and S F Trevino, Phys. Rev. Lett. **54** (1985) 193 & B Alefeld, I S Anderson, A Heidemann, A Magerl and S F Trevino, J. Chem. Phys. **76** (1982) 2758
81. M W G Withall and G A Gehring, J. Phys. C **20** (1987) 1619
82. M Prager, J Stanislawski and W Häusler, J. Chem. Phys. **86** (1987) 2563
83. S Clough, New Scientist 24 March (1988) 37, S Clough, Ber. Bunsenges. Phys. Chem. **93** (1989) 1182 & S Clough, Mol. Phys. **68** (1989) 1255
84. A Heidemann, K J Abed, C J Barker and S Clough, Z. Phys. B **66** (1987) 355
85. A Inaba, H Chihara, J A Morrison, H Blank, A Heidemann and J Tomkinson, J. Phys. Soc. Japan **59** (1990) 522
86. H Friedrich, K Guckelsberger, R Scherm and A Hüller, J. Phys. C **14** (1981) L147
87. A Hüller and M Prager, Solid. State Commun. **29** (1979) 537
88. B Krebs, G Henkel and M Dartmann, Acta Cryst. C **45** (1990) 1010
89. D Smith, J. Chem. Phys. **68** (1978) 619, & **82** (1985) 5133, & **92** (1990) 4669.
90. M Prager, W Press, B Alefeld and A Hüller, J. Chem. Phys. **67** (1977) 5126 & M Prager, A M Raaen, and I Svare, J Phys C: Solid State Phys. **16** (1983) L181
91. A Heidemann, K J Lushington, J A Morrison, K Neumaier and W Press, J. Chem. Phys. **81** (1984) 5799
92. S Grondey, M Prager and W Press, J.Chem. Phys. **86** (1987) 6465, & **85** (1986) 2204
93. W Langel, M Prager, H W Fleger, E Knozinger, H J Lauter, H Blank & C J Carlile, J. Chem. Phys. to be published (1993)
94. F Leclercq, P Damay and P Chieux, J. Phys. Chem. **88** (1984) 3886
95. M Prager and W Langel, J. Chem. Phys. **90** (1989) 5889
96. Y Ozaki, Y Kataoka and K Okada, J. Chem. Phys. **73** (1980) 3442
97. T Yamamoto, Y Kataoka and K Okada, J. Chem. Phys. **66** (1977) 2701
98. M J Frisch et al., *GAUSSIAN90*, Gaussian Inc., Pittsburgh, PA, (1990)
99. A I Kitaigorodskii, Acta Cryst. A **31** (1965) 448
100. B R York and S A Solin, Phys. Rev. B **31** (1985) 8206
101. D A Neumann, H Zabel, J J Rush, Y B Fan and S A Solin, Phys. Rev. B **30** (1985) L761
102. Y B Fan, S A Solin, D A Neumann, H Zabel and J J Rush, Phys. Rev. B **36** (1987) 3386
103. C J Carlile, I McL Jamie and J W White, to be published
104. H James and T Keenan, J. Chem. Phys. **31** (1959) 12
105. B Asmussen, M Prager, W Press, H Blank and C J Carlile, J. Chem. Phys. **97** (1992) 1332
106. N Le Calvé, D Cavagnat, and F Fillaux, Chem. Phys. Letts. **146** (1988) 549
107. K J Abed, S Clough, C J Carlile, B Rosi and R C Ward, Chem. Phys. Letts. **141** (1987) 215
108. F Fillaux and C J Carlile, Chem. Phys. Letts. **162** (1989) 188
109. F Fillaux, C J Carlile and G J Kearley, Phys. Rev. B **44** (1991) 12280
110. F Fillaux, C J Carlile, A Heidemann, J C Cook, G J Kearley and D S Sivia, to be published
111. C J Carlile, R M Ibberson, F Fillaux and B T M Willis, Z. Krist. **193** (1990) 243
112. R K Thomas, *Neutron Scattering from Adsorbed Systems,* Progr. Solid State Chem. **14**, 47 (Pergamon, New York, 1982) & P C Ball, A Inaba, J A Morrison, M V Smalley and R K Thomas, J. Chem. Phys. **92** (1990) 1372
113. J P Beaufils, T L Crowley, T Rayment, R K Thomas and J W White, Mol. Phys. **44** (1981) 1257
114. J M Nicol, J Eckert and J Howard, J. Phys. Chem. **92** (1988) 7117, J Eckert, *Cong. Int. Union of Crystallography,* Bordeaux 1990, C-298 & J Eckert, G J Kubas and A J Dianoux, J. Chem. Phys. **88** (1988) 466
115. J C Cook, W Petry, A Heidemann and B Frick, ILL report 91COO6T (1991)